MODERN METHODS OF EXOPLANET DETECTION

Kevin Hoy, Joshua Kingsbury, Avidaan Srivastava, Logan Steele

1. Motivation

Ever since Wolszczan and Frai made the first definitive discovery of exoplanets in 1992, astronomers have been looking for ways to make other such discoveries. The primary reason being our solar system is just one of many such planetary systems that exist in the universe and analyzing these exoplanets in turn helps in understanding our solar system and its planets better. It enhances our understanding of the various trends in planet formation around different stars and make comparisons to our solar system in order to determine if the existence of a planet like Earth was just a fluke or are there other worlds where similar conditions can be achieved for life to prosper.

Over the years, the exoplanet detection methods have progressed leaps and bounds and today we have over 4000 confirmed detected exoplanets (NASA, 2022), all of which have enhanced our knowledge about the Universe as a whole. However, not all of these methods work all the time and sometimes require very specific conditions for orientation of planet's orbit, planet's distance from the star or even the thermal emission of the planet. Which is why it is important to understand the caveats associated with these detection methods to minimize selection bias.

2. Methods

In this report the physics behind the three main methods of exoplanet detection: (1) Radial Velocity, (2) Transits and (3) Direct Imaging are discussed in detail along with estimates about the limits of today's cutting-edge technology and if it was our solar system being observed, would Jupiter be detected as an exoplanet around the Sun.

2.1 Radial Velocity

This technique involves finding the relation between the radial velocity of an object in orbit and its mass assuming 2-body Keplerian motion (Lovis and Fischer, 2010). The equations below explain said relation:

$$P^2 = 4\pi^2 \times \frac{a^3}{GM_*} \quad \text{--- (1)}$$

$$K = v_p \times sin(i) = 2\pi \left(\frac{M_p}{M_*}\right) \times \sqrt{\frac{GM_*}{a}} \times sin(i) \quad \text{--- (2)}$$

Here P refers to the planet's period of revolution around the star, a is the semi-major axis of the orbit, G is the universal gravitation constant, M_* is the mass of the star, M_p is the mass of the orbiting planet, v_p the orbital speed of the planet and i is the angle of inclination of the orbit from

our plane of view. Equation (1) is Kepler's third law and can be used to derive Equation (2) which gives the value if the planet's redial velocity signal, also called the RV semi-amplitude (K) (Lovis and Fischer). Usually, the angle of inclination is unknown and therefore a measurement of: $M_p \sin (i)$ is made and an estimate of the 'minimum planet mass' is made. The state-of-the-art detection is currently the most suitable for detecting planets around unevolved-G, late-K and M stars due to the smaller noise signal and low mass of these stars amplifying the RV signals of the orbiting planets. The current latest and greatest equipment is capable of measuring RV signals as low as 0.5 m/s (Pepe et al., 2020) with a mass detection limit of 0.5 M_{Sun}.

2.2 Transits

This method of observation relies on the principle of eclipses that Dr. Joshua Winn defines as "the obscuration of one celestial body by another" (Winn, 2010). The most important requirement to effectively use this technique is that the inclination of the planet's orbit around the star needs to be 'near edge-on'. Below are some important equations needed to make calculations using this technique:

$$P_{Transit} = \frac{R_p + R_*}{a} \text{ --- (3)}$$

$$\delta = \left(\frac{R_p}{R_*}\right)^2 \text{ --- (4)}$$

$$SNR = \frac{\delta}{\sigma_{CDPP}} \times \sqrt{\frac{n_{tr} t_{dur}}{b}} \text{ --- (5) (Christiansen et al., 2012)}$$

In equation (3), $P_{Transit}$ represents the probability of a transit being detected, R_p, R_* and a once again represent the radii of the planet and star respectively and the semi-major axis of the orbit. The ratio of the cross-sectional areas of the planet and star are given in equation (4) with δ being called the depth of transit. Equation (5) gives the signal to nouse ratio (SNR) and its relation to δ, sensitivity limit (σ_{CDPP}), number of transits during the observation time span ($n_{tr} \sim 90$ days for K2), duration of full transit (t_{dur}) and binning interval (b). This depth of transit is the important quantity that must be significant enough for the state-of-the-art detectors to measure. It heavily favors large planets (comparable to Jupiter) with short revolution periods (of the order of a few days). The best depth of transit detection limit of today's equipment is given by the Kepler telescope (K2 more specifically) as 12 parts per million (ppm).

2.3 Direct Imaging

This detection method involves directly observing the planet around a star by artificially suppressing the light from the central star using techniques such as a rectangular mask coronagraph or angular differential imaging. Direct Imaging heavily favors young, hot, self-luminous planets as their high temperature gives them a strong detectable flux and 'Their large distances from their planet stars makes them easier to see in the halo of atmospherically or

instrumentally scattered star light' (Traub and Oppenheimer, 2010). Below are the important equations for this technique:

$$f_R = \frac{\pi R_p^2}{4\pi a^2} \times A \text{ --- (6)}$$

$$B_v(T) = \frac{2hv^3}{c^2} \times \frac{1}{e^{\frac{hv}{k_B T}} - 1} \text{ --- (7)}$$

$$f_c = p\varphi \frac{R_p^2}{a^2} + \frac{R_p^2}{R_*^2} \times \frac{e^{\frac{hv}{k_B T_*}} - 1}{e^{\frac{hv}{k_B T_p}} - 1} \text{ --- (8)}$$

$$\theta \sim 1.22 \frac{\lambda}{D} \text{ --- (9)}$$

Here, f_R is the starlight reflected by the planet and is directly related to the albedo (A). Equation (7) shows the Planck function which is a measure of the thermal emission of a body and depends on the Planck's constant (h), speed of light (c), frequency (v), Boltzmann constant (k_B) and temperature (T). Assuming that both the star and the planet emit thermal emission, equation (8) shows the Star-Planet contrast and its relation to T_p, T_* geometric albedo (p) and phase (φ) which are the temperatures of the planet and the star respectively. Another criterion for using this technique is that the planet needs to be identified as a distinct source by the telescope and equation (9) shows the Rayleigh limit with λ acting as the wavelength over which the telescope operates, and D is the telescope's diameter. The Thirty Meter Telescope's (TMT) proposed Second Earth Imager instrument is the state-of-the-art equipment and is capable of looking at contrast of 8 x 10^{-8} at 0.01 arcseconds (Matsuo et al., 2012).

3. Results

The first set of results (Figure 1 a, b, c, d) involves extracting exoplanet data from NASA's Exoplanet Archive (NEA) and overplot the solar system planets on them to get a better understanding of how common it is to detect similar planets. It can be clearly seen that most of the detected planets are above the sensitivity lines for their respective detection methods and the few outliers can be explained by statistical uncertainties or, a different method was used to obtain that data.

Additionally, there is a considerable decrease in the planets discovered through RV signals in the plots featuring 'Radius' on one of the axes (Figure a and b). This is because as seen from equations (1) and (2), there is no R_p term and hence it is difficult to derive it from the data. The majority of the Radius data as seen from the plots is obtained from the Transits technique which lets us directly get a measure of the planet's radius as seen from equation (4). Data for masses of planets detected through Transits cannot be obtained directly, which is why the Transit sensitivity lines are missing from Figures c and d. The planets detected through Direct Imaging are few and far between and are located in the top right corner in each of the graphs and the dimensions of the 'box' are determined by the detection limits of the current equipment.

For the purposes of this project, the special case of a Jupiter-like planet around a sun-like star was chosen to better understand the limitations and capabilities of the state-of-the-art detection equipment for the three methods discussed in the previous section. Jupiter has a semi-major axis of 5.2 AU, mass of 1.898 x 10^{27} kg and for an edge-on orbit ($i = 90°$) the derived K value for the RV signal would be 12.46 m/s, which is higher than the state-of-the-art detector limit of 0.5 m/s. This means that the current RV equipment is a very good way to detect Jupiter-like planets around Sun-like stars.

The K2 instrument is sensitive to a planet 1/30 the radius of Jupiter around a sol-type star but observing conditions might suggest 1/5 the radius of Jupiter is a bit more reasonable. Interestingly, the smallest planet found by K2 so far has a radius of 0.055 R_J (Radius of Jupiter), just above the baseline estimate sensitivity of 0.034 R_J.

Another important consideration is the probability that a planet's orbit causes it to eclipse its star. Since the ecliptic plane is oriented randomly with respect to us, most planets that exist cannot be detected using the transit method. For the specific case of Jupiter-like planet around a Sun-like star, the probability of K2 making the detection is 0.09862%. So, even though the equipment can theoretically detect Jupiter, the likelihood of that happening it quite low.

Direct Imaging is the third and final detection technique discussed in this report and the future benchmark will be set by the TMT. Assuming geometric albedo is constant and that the phase is $\pi/2$, Jupiter's signal at its peak of emission (23 microns) is 10^{-6} and the signal at Sun's peak (0.5 microns) is 10^{-9}. This falls well within the detection range of the Second Earth Imager (SEIT) instrument listed in section 2.3. To actually make the observation, the equipment should have high enough angular resolution as well as a good enough detector to measure the brightness contrast. The TMT can theoretically detect a Jupiter-like planet around a Sun-like star if it's within 32 parsecs of Earth, but the SEIT instrument only allows such a measurement to happen within 9 pc. This means that the instrument cannot keep up with the full capabilities of the telescope.
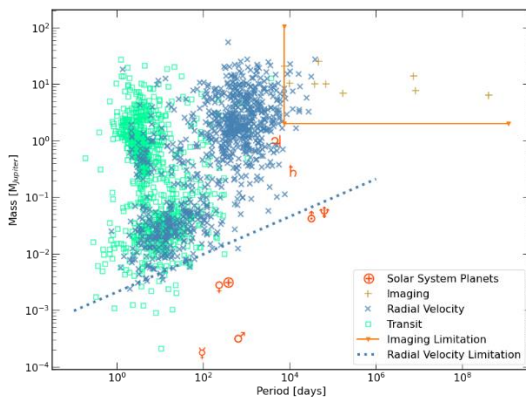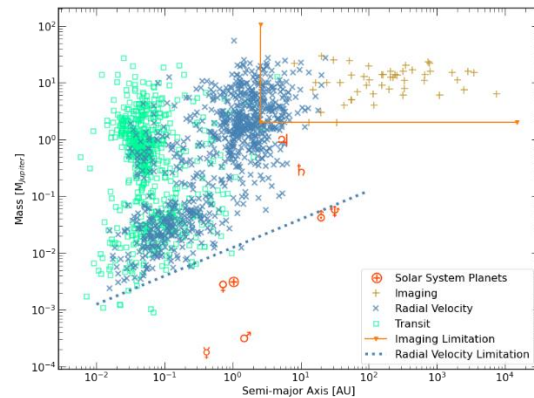
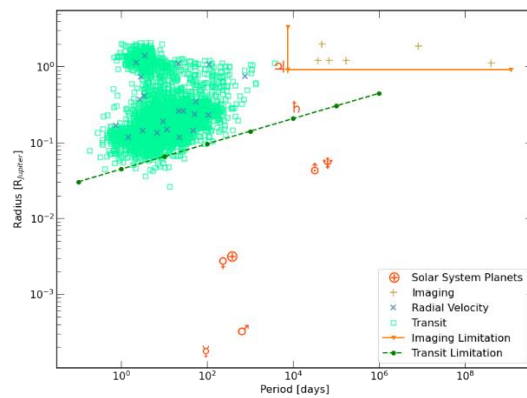a)   b)
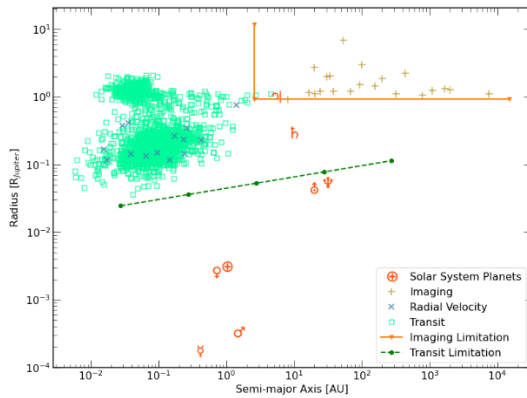
c)   d)

Figure 1: a) Mass-Period plot of all the NEA planets with the sensitivity line for RV and Direct Imaging; b) Mass-Semimajor Axis plot of all the NEA planets with the sensitivity line for RV and Direct Imaging; c) Radius-Semimajor Axis plot of all the NEA planets with the sensitivity line for Transit and Direct Imaging; d) Radius-Semimajor Axis plot of all the NEA planets with the sensitivity line for Transit and Direct Imaging

4. Conclusion

The current state-of-the-art equipment provides varied degrees of success and precision if a Jupiter-like planet around a Sun-like star was to be detected. The Radial Velocity method has a detection limit of 0.5 m/s and can comfortably detect the planet in this case. If Transits were used instead, then there's only a 0.09862% chance to catch Jupiter in-transit and if such a condition was obtained, then the planet would be detected. Finally, Direct Imaging can indeed detect the planet if SEIT is used, and the target planet is within 9 pc of the Earth, which is a very short distance.

5. Contributions

This report was done in collaboration by Kevin Hoy, Joshua Kingsbury, Avidaan Srivastava and Logan Steele. The work was divided amongst the members and the project was completed together as a team. The specific contributions of each member of the team are listed below:

Kevin Hoy: Analysis of Direct Imaging detection method
Joshua Kingsbury: Analysis of Transits detection method
Avidaan Srivastava: Writing of the report
Logan Steele: Analysis of Radial Velocity detection method and in-class presentation

6. References:

NASA, 2022. https://exoplanets.nasa.gov/faq/6/how-many-exoplanets-are-there/

Lovis and Fischer, 2010. *Radial Velocity Techniques for Exoplanets*. Exoplanets. Project Muse.
Edited by Sara Seager.

Pepe et al., 2020. *ESPRESSO@VLT -- On-sky performance and first results*. arXiv.org.
Retrieved February 1, 2022. https://arxiv.org/abs/2010.00316

Winn, J., 2010. *Exoplanet Transits and Occultations*. Exoplanets. Project Muse. Edited by Sara
Saeger.

Traub and Oppenheimer, 2010. *Direct Imaging of Exoplanets*. Exoplanets. Project Muse. Edited
by Sara Seager.

Christiansen et al., 2012. *The Derivation, Properties and Value of Kepler's Combined
Differential Photometric Precision*. https://arxiv.org/pdf/1208.0595.pdf

Matsuo et al., 2012. Second-Earth imager for TMT (SEIT): concept and its numerical simulation.
SPIE. https://www.spiedigitallibrary.org/conference-proceedings-of-
spie/8446/84461K/Second-Earth-imager-for-TMT-SEIT--concept-and-
its/10.1117/12.926039.short?SSO=1